Journal of Engineering, Project, and Production Management
2027, 17(2), 2025-310

Propagation Characteristics of 5G Electromagnetic Waves in Coal Mine Tunnels by Integrating SBR/IM and GA-SVM

Zhiguo Wen
Director, Hydraulic Power Research Institute, the Intelligent Equipment Branch of China Coal Technology and Engineering Group Co., Ltd., Beijing, 100013, China,
Email: Zhiguo_wen@outlook.com

Engineering Management
Received December 12, 2025; revised February 2, 2026; August 2, 2026; accepted October 25, 2026
Available online November 5, 2026

Abstract: With the advancement of intelligent construction in coal mines, 5G communication technology has become a key support for underground core networks. To analyze the electromagnetic wave propagation characteristics of 5G signals in coal mine tunnels, an innovative method that integrates the Shooting and Bouncing Ray/Image Method (SBR/IM) with a Genetic Algorithm-Optimized Support Vector Machine (GA-SVM) is proposed. The SBR/IM method is used to construct a three-dimensional electromagnetic simulation model of the tunnel, simulating multi-path propagation and generating high-precision training data. The GA-SVM algorithm is then employed to intelligently correct and predict signal path loss, enhancing model accuracy and generalization capability. Experimental results under typical tunnel conditions show that the proposed fusion model achieves a maximum path loss of only 63 dB at 0.2 m wall thickness, which is 51 dB lower than that of the traditional Floating Interception (FI) model. Moreover, the signal-to-noise ratio remains above 0 dB within 225 m, significantly outperforming the FI model. At a wall thickness of 0.3 m, the path loss of the fusion model is 72 dB. Additionally, the fusion model exhibits a received signal strength index of -68 dBm, a coherent bandwidth of 25 MHz, a throughput of 320 Mbps, and a delay as low as 15ms, all of which are superior to those of comparative models. The proposed hybrid method effectively enhances the propagation performance of 5G signals in coal mine tunnels, reduces path loss, improves signal quality, and provides a valuable approach for studying electromagnetic wave propagation in such environments.

Keywords: Shooting and bouncing ray/image method (SBR/IM); genetic algorithm-optimized support vector machine (GA-SVM); electromagnetic wave propagation characteristics; coal mine roadway; fusion model.

Copyright © Journal of Engineering, Project, and Production Management (EPPM-Journal).
DOI 10.32738/JEPPM-2025-310

1. Introduction

With the deepening of intelligent construction in the coal industry, 5G communication technology has become the key to building the core network underground in coal mines due to its high bandwidth, low latency, and wide connectivity. However, the complex and specialized environment of coal mine tunnels, with their narrow, enclosed geometric structures, rough, uneven wall surfaces, and densely distributed obstacles, causes significant reflection, diffraction, and scattering of 5G electromagnetic waves during propagation. This leads to significant path loss, multi-path fading, and signal distortion, severely restricting the implementation of high-quality wireless communication (Lei et al., 2024; Kurbah and Ahmed, 2024). Therefore, accurately predicting the propagation characteristics of 5G electromagnetic waves in coal mine tunnels has crucial theoretical significance and engineering value for the scientific planning, coverage optimization, and reliability improvement of underground networks. Currently, research methods for predicting radio wave propagation mainly include empirical models based on statistical regression, deterministic models based on electromagnetic physics theory, and data-driven machine learning models. Although empirical models are computationally simple, their accuracy is limited, and their generalization ability is weak. Deterministic models have clear physical meaning and high accuracy, but they are computationally complex and rely on fine-grained environmental modeling. Machine learning models are good at mining nonlinear relationships in data, but their performance heavily relies on hyperparameter optimization and training data quality. A single model often struggles to achieve an ideal balance between computational efficiency, prediction accuracy and generalization ability (Liu et al., 2025; Yu et al., 2024).

At present, multiple studies have conducted more in-depth analyses. For example, Wei et al. (2024) explored the

difficulty in accurately assessing the electromagnetic radiation level of 5G base stations due to complex environmental factors. Through field monitoring and correlation analysis in different typical scenarios, they revealed that transmission distance, user density, and building reflection superposition are key factors affecting radiation power density. This provides important empirical evidence for understanding the environmental behavior of base station radiation and lays a theoretical foundation for the scenario-based application of risk management. Li et al. (2024) proposed a miniaturized frequency-selective absorber based on a complementary bandpass Frequency Selective Surface (FSS) to address the urgent need for miniaturization and electromagnetic compatibility of radio frequency front-end devices in 5G systems. The meandering circular resistive layer is integrated with a complementary Jerusalem cross FSS structure and loaded with lumped elements to optimize impedance matching. A high transmission rate of 87.5% and broadband absorption characteristics are achieved in the 2.6 GHz band, significantly improving the device's performance in complex electromagnetic environments. Shi et al. (2024) proposed a new machine learning-based electromagnetic radiation intensity estimation method to solve the high cost, low efficiency, and difficulty in large-scale application of traditional electromagnetic radiation measurement methods. This method integrates multi-dimensional characteristics, such as antenna power, distance, number of terminals and environmental complexity, to train the prediction model and estimate the near-earth electric field intensity with high accuracy, providing low-cost, highly reliable data support for scientific site selection and efficient supervision of 5G base stations.

Although significant progress has been made in the empirical measurement of 5G electromagnetic radiation, the development of absorbing materials, and intelligent prediction methods, there are still certain limitations in existing research. Most studies focus on on-site measurements in a single scenario, lack in-depth exploration of complex tunnels and other specialized enclosed environments, or focus on hardware design and algorithmic prediction. They fail to integrate high-precision electromagnetic simulation with powerful machine-learning optimization capabilities, limiting their ability to generalize and their prediction accuracy in complex and changing environments. The aim of this study is to propose and validate a fusion model that combines SBR/IM electromagnetic simulation with GA-SVM machine-learning optimization to enhance the analysis and prediction of 5G signal propagation characteristics in coal mine tunnels. The research focuses on three core issues: how to use SBR/IM to construct a high-precision tunnel propagation model, how to optimize GA-SVM to achieve intelligent prediction using simulation data, and whether the proposed fusion model outperforms traditional methods on key performance indicators. Therefore, this article assumes that SBR/IM can effectively simulate multipath effects in tunnels, that GA-SVM can significantly improve prediction accuracy using simulation data, and that the fusion model offers significant advantages in overall performance, including path loss, signal-to-noise ratio, and throughput. The study will validate these hypotheses through comparative experiments.

2. Methodology

2.1. Modeling of Coal Mine Channel Communication Based on SBR/IM

The SBR/IM signal-tracking method can determine the propagation path of electromagnetic waves in complex environments. This method can significantly enhance the transmission positioning analysis of electromagnetic wave signals. The SBR/IM method virtually emits a large number of rays from the transmitting antenna into a complex tunnel environment, and efficiently calculates the multiple reflections and diffraction paths of the rays on the tunnel walls and obstacles using the mirror method, thereby accurately predicting the multi-path propagation characteristics of radio waves (Huang et al., 2024; He et al., 2024). The operation process of SBR/IM is shown in Fig. 1.

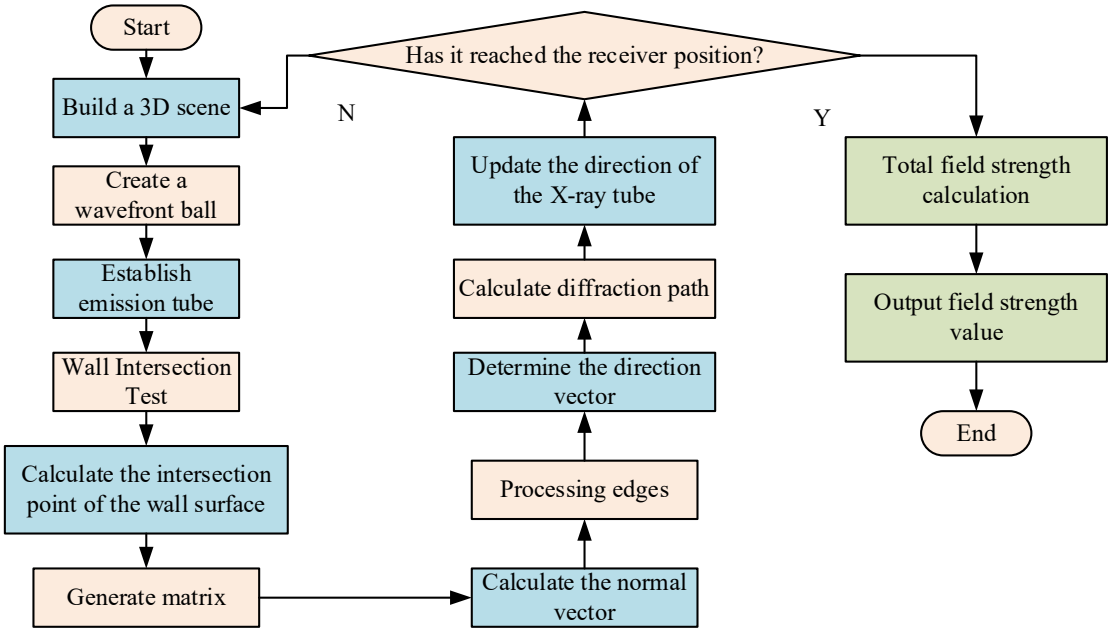


Fig. 1. BR/IM operation process

In Fig. 1, SBR/IM first constructs a three-dimensional scene with geometric and electromagnetic properties, including

walls and edges. Subsequently, a wavefront sphere is created by treating the source as a spherical wavefront and establishing an emitter ray tube to form a beam of rays representing the direction of wave propagation. Wall intersection tests are conducted to calculate the intersection points of each ray with all walls in the environment. An intersection matrix is generated that records information such as the position of each intersection point and the incident angle. If the ray intersects the wall, the wall's normal vector needs to be calculated, and any possible edges of the wall need to be processed. During the process, the radiation tube's direction vector after reflection or diffraction is determined, and the diffraction path of the straight beam is calculated using the theory of uniform diffraction to update the radiation tube's direction. All effective rays are finally received at the receiving point, allowing determination of whether they have reached the receiver position. Coherent superposition is performed using the amplitude, phase, and path delay of each ray to compute the total field strength and output the synthesized field strength at the receiving point. When locating signals, the diffraction signal reception is given by Eq. (1) (Zhu et al., 2024).

$$(n, m, z + \frac{(z_a - z_b)\sqrt{(n-n_b)^2 + (m-m_b)^2}}{\sqrt{(n-n_b)^2 + (m-m_b)^2} + \sqrt{(n-n_a)^2 + (m-m_a)^2}}) \tag{1}$$

In Eq. (1), n, m, and z represent the horizontal coordinates of the diffraction point. n_b, m_b, and z_b represent the coordinates of the fixed source point. n_a, m_a, and z_a represent the coordinates of the predetermined field point, respectively. If the final calculated result is outside the transmission and reception points, it is unreasonable to define the current diffraction point. If it is between the transmission and reception points, the diffraction effectiveness depends on the presence of obstacles, which is invalid. The SBR/IM method is a process for transmitting wireless signals in different directions from a transmission point, using light rays to detect signal changes in the tunnel. The field strength carried by the initial rays during signal transmission is given by Eq. (2) (Wang et al., 2024; Guo et al., 2025).

$$E_0 = C * \frac{\sqrt{P_t * G_t}}{d} * e^{-jkd} \tag{2}$$

In Eq. (2), E_0 represents the initial field strength carried by the radiation tube. The C is a constant. The P_t denotes the transmission power of the transmitting antenna. The G_t means the gain of the transmitting antenna. The d refers to the radial distance from the transmitting antenna to the initial position of the radiation tube. The k represents the wavenumber. The j represents the imaginary unit. During the launch process, diffraction occurs when the trajectory encounters obstacles. The diffraction field strength is shown in Eq. (3) (Gai et al., 2024; Su et al., 2024).

$$E_d = E_t * D * A(s, s') * e^{-jks} \tag{3}$$

In Eq. (3), E_d represents the electric field strength after diffraction. The E_t represents the incident electric field strength. The E_t represents the diffraction coefficient. The $A(s, s')$ represents the spatial attenuation factor. The s represents the distance from the diffraction point to the observation point. The s' represents the distance from the source point to the diffraction point. The change in total field intensity after diffraction reaches the receiving point is shown in Eq. (4) (Zhang et al., 2025).

$$E = \sum_i [|E_i| * e^{-j(kd_i + \phi_0)}] \tag{4}$$

In Eq. (4), E represents the total electric field strength at the receiving point. The E_i represents the electric field amplitude of the i th path. The d_i means the propagation distance of the i th path. The ϕ_0 represents the initial phase. The impulse response of the signal channel is obtained through the relationship between field strength and signal transmission, as shown in Eq. (5) (Ma et al., 2024; Bao et al., 2024).

$$h(t) = \sum_i a_i * \gamma(t - t_i) \tag{5}$$

In Eq. (5), $h(t)$ represents the channel impulse response. The a_i represents the amplitude coefficient of the i th path. The t_i represents the propagation delay of the i th path. The $\gamma(t - t_i)$ represents the Dirac impulse function. Therefore, based on the actual field strength and signal changes, the coal mine tunnel is modeled.

The signal transmission source is set on the roof of the office building or at the top of the derrick in the mining area, at a height of 20-30 m, as is typical for mining facilities. Several signal reception sources are set up and placed along the line-of-sight and non-line-of-sight routes. On each path, the distance between the two signal reception sources is 5-10 m to simulate mobile terminals or fixed monitoring points. The specifications of the transmitting and receiving sources are specific frequency bands suitable for mining area coverage and mining area-specific frequency bands.

2.2. Propagation Characteristics of 5G Electromagnetic Waves in Coal Mine Tunnels Based on GA-SVM

After modeling signal transmission in coal mine tunnels using SBR/IM, GA-SVM is used to accurately detect 5G

electromagnetic signals and perform path-loss correction analysis. Given the many factors that affect signal propagation throughout the receiving process, the most influential factors are selected as input data for GA-SVM training to reduce propagation losses. The effective reflection coefficient for tunnel walls is given by Eq. (6).

$$R_r = \rho_s * R \tag{6}$$

In Eq. (6), R_r represents the Fresnel reflection coefficient of a smooth surface. The ρ_s represents the roughness attenuation factor. The attenuation factor is shown in Eq. (7).

$$\rho_s = \exp[-2(\frac{2\pi\sigma_h \cos\theta_i}{\lambda})^2]] \tag{7}$$

In Eq. (7), σ_h refers to the Root Mean Square (RMS) roughness of the surface height. The θ_i denotes the angle of incidence of the electromagnetic wave. The λ means the wavelength of the 5G signal. The formula for correcting the roughness field strength during signal propagation is given by Eq. (8) (Ren et al., 2024).

$$E_r = R_r * \frac{\sqrt{G}}{d} e^{-jkd} = (\rho_s * R) * \frac{\sqrt{G}}{d} e^{-jkd} \tag{8}$$

In Eq. (8), E_r represents the field strength after roughness correction. In the actual roughness impact analysis, the tunnel wall roughness is measured and incorporated into the formula to accurately calculate the 5G signal's propagation characteristics in the tunnel. The influence of tunnel wall roughness is shown in Eq. (9) (Srinivas et al., 2025).

$$L_R = 8.636\pi^2 \Delta h^2 z(\frac{1}{a^4} + \frac{1}{b^4}) \tag{9}$$

In Eq. (9), L_R represents the additional path loss caused by roughness. The Δh represents the RMS roughness of the tunnel wall surface. The z represents the transmission distance between the transmitter and receiver. The a and b represent the half-width and half-height of the tunnel cross-section, respectively. The path loss of signal propagation is corrected through the GA-SVM algorithm. The GA-SVM flow is shown in Fig. 2.

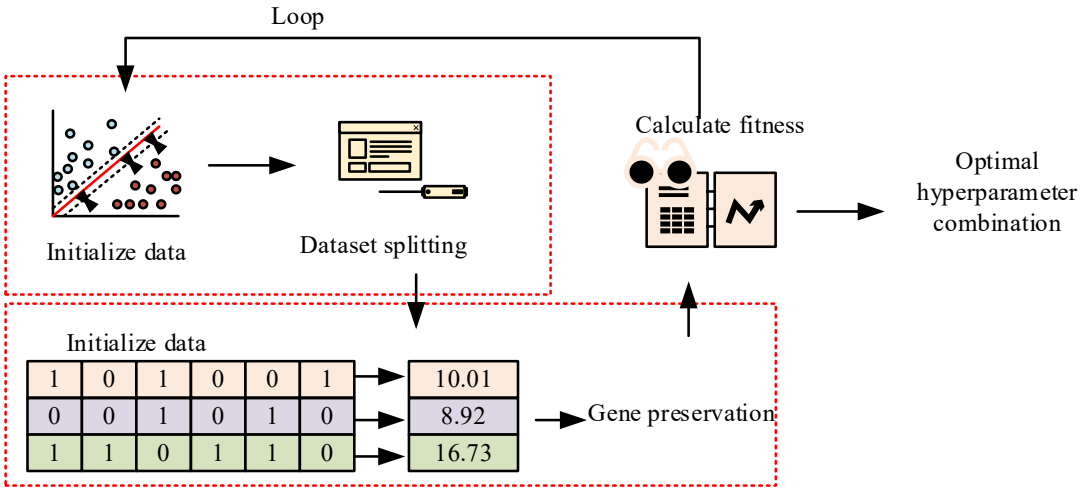


Fig. 2. GA-SVM flow

In Fig. 2, GA-SVM first initializes the data, then divides the dataset into training and testing sets. The Genetic Algorithm (GA) first initializes the population. Each individual in the population encodes the key hyperparameter combination of the SVM. Subsequently, the model calculates each individual's fitness and enters the GA's optimization cycle to perform selection operations based on fitness. Finally, the optimal hyperparameter combination obtained through evolution is assigned to the SVM model, and the model's final performance is evaluated on the test set to complete the modeling process. After changing the channel signal reception through SBR/IM, GA-SVM is used to predict the channel signal. Fig. 3 presents the process for predicting channel signal data.

In Fig. 3, the GA-SVM model first collects data from 5G channel signals, then performs data preprocessing and feature extraction to construct a feature vector set containing key features such as distance and tunnel section parameters. Then, the GA and SVM processes are used to initialize the population of encoded parameter combinations. By calculating the cross-validation accuracy of the SVM model on the training set for each parameter set, iterative selection, crossover, and mutation operations are performed to evolve the population until the maximum number of iterations is reached or the fitness meets the accuracy requirements. The optimal hyperparameter combination is output. After training the SVM model with optimal parameters, the signal propagation characteristics are predicted on the test set, and performance is evaluated by calculating metrics such as mean squared error. If the prediction accuracy meets the requirements of practical applications,

the current best tunnel channel signal data is output. If it does not meet the requirements, feedback adjusts the GA parameters to reoptimize until a reliable prediction model that meets the performance goals is obtained. In data processing, the first step is to ensure that the algorithm can receive the data. Therefore, during training, the data needs to be preprocessed. The data preprocessing process is denoted in Fig. 4.

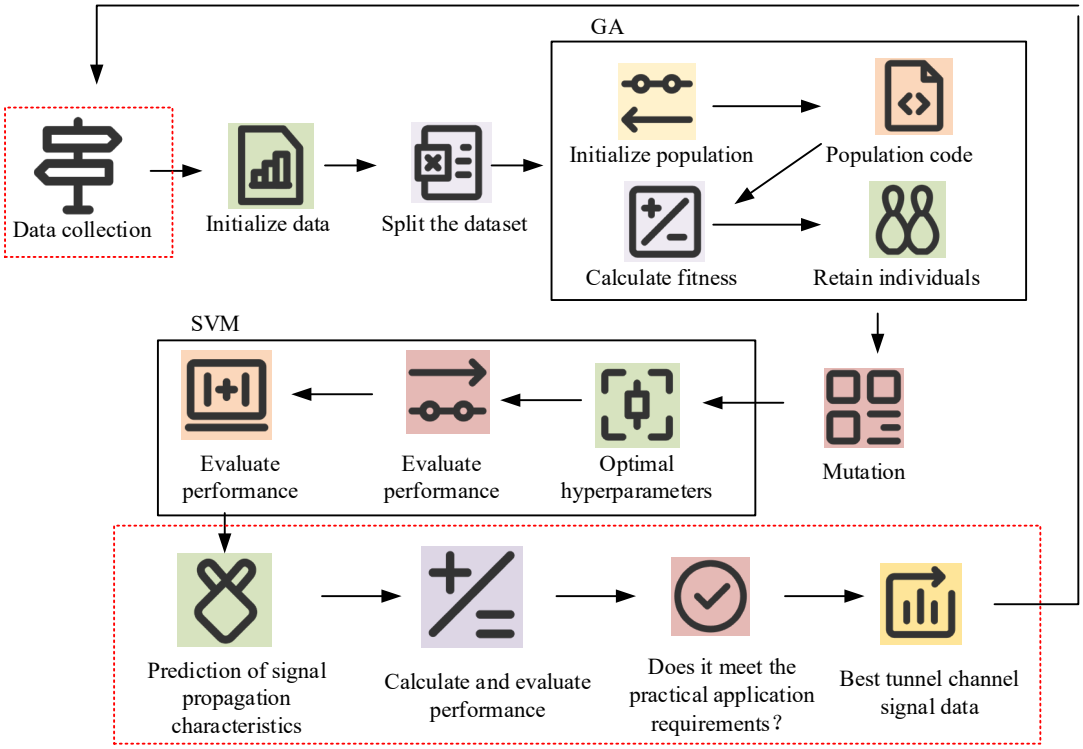


Fig. 3. Prediction and analysis process of channel signal data

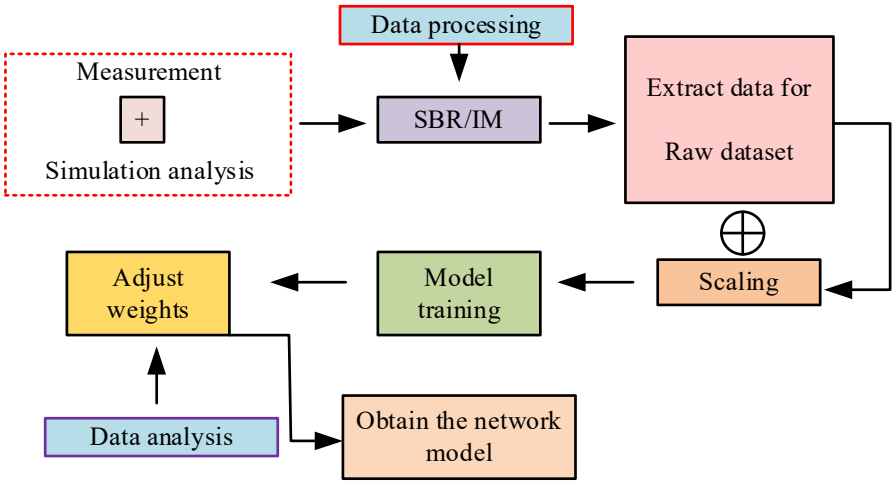


Fig. 4. Data preprocessing process

In Fig. 4, during data preprocessing, the channel signal data must be measured and simulated for analysis. This process is mainly achieved through channel modeling using the SBR/IM method. The raw dataset is obtained through actual measurement or simulation, and data pairs are then extracted for training. Subsequently, the data is subjected to scale transformation to eliminate the influence of dimensionality. The transformed data is fed into the GA-SVM model for training. The network output is adjusted to approximate the target by adjusting the weights. After the training is completed, the trained neural network model is obtained.

2.3. Construction of 5G Communication Network in Coal Mine Tunnels

To analyze the electromagnetic wave propagation characteristics of coal mine tunnels, it is necessary to build a 5G communication network. In addition to communication transmission, it is necessary to analyze the processes of signal reception and electromagnetic wave propagation. Due to the various factors that must be considered in 5G communication networks, ordinary equipment is also prone to damage in coal mine environments. Therefore, a safe and feasible 5G communication network is constructed to enable long-term operation while ensuring network security. The structure of the

5G communication network in coal mine tunnels is shown in Fig. 5.

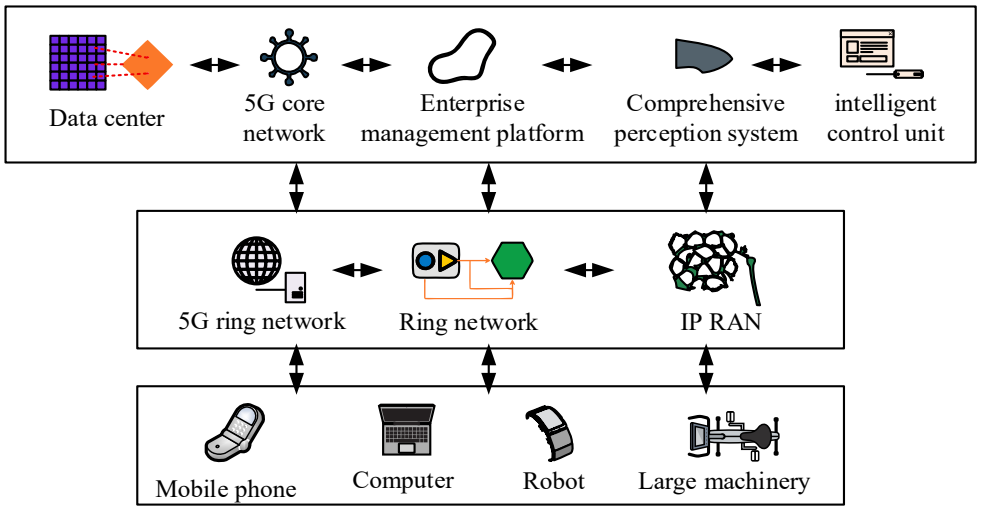


Fig. 5. Composition of 5G communication network structure in coal mine tunnels

In Fig. 5, the entire 5G mine communication structure is divided into multiple layers, including the top application layer of the data center, the 5G core network, the enterprise management platform, the comprehensive perception system, the intelligent control unit, and the execution system. The second layer is the public network, mainly including the 5G ring network, which can adopt a high reliability ring topology and be carried by IP Radio Access Network (IP RAN) technology to connect access layer network devices. Finally, there are communication substations and various terminals, including mobile office equipment such as smartphones, computers and tablets, as well as key production equipment such as robots and large machinery. After completing the overall network construction, the mine's ring network system is designed, as shown in Fig. 6.

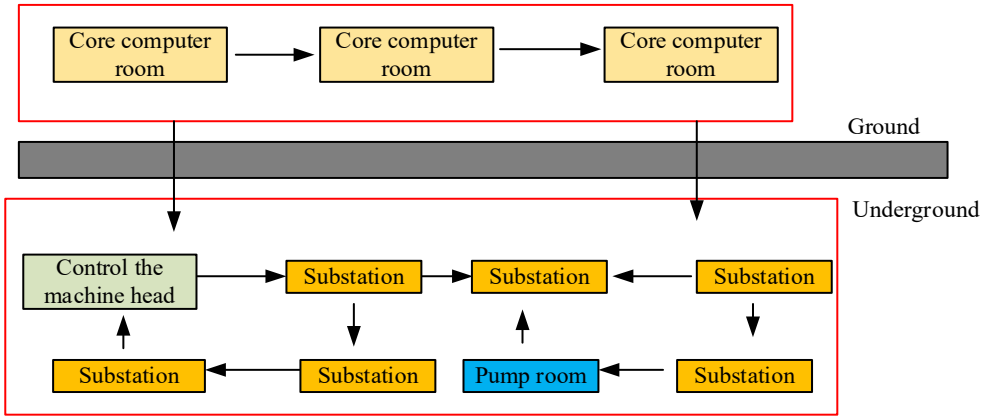


Fig. 6. Mine ring network system

In Fig. 6, the entire ring network system is equipped with two core computer rooms on the ground to ensure high availability of core control and data processing. Then, multiple different substations and water pump rooms are set up in the main ring network under the coal mine roadway. Core computer room 1 controls the machine head and substation, while the machine head, in turn, controls the water pump room and the mining area substation. The other core computer room controls the central substation. The entire ring network is intricately interconnected, forming a complex control network.

3. Results and Analysis

3.1. Model Communication Reception and Propagation Effect Testing

To analyze the propagation characteristics and path loss of 5G signals in coal mine tunnels, a 5G communication system was designed. The working frequency center of the 5G communication system was 3.4 GHz, and the transmission bandwidth was set to 80 MHz. The transmitting and receiving devices all used omnidirectional, vertically polarized antennas installed at the center of the tunnel section, which was the geometric center in the height and width directions. The transverse profile at this height was selected as the region for signal field-strength analysis. The antenna gain was adjusted to 3 dBi, the transmission power was set to 33 dBm, and the receiver sensitivity was defined as -118 dBm. The simulated roadway width and height were 4m and 5m, respectively, and the model length was 2,000m. The relative dielectric constant of the tunnel wall was 5, the conductivity was 0.66 S/m, and the average height of the tunnel wall was 0.2m. Simultaneously, it simulated the height of the second tunnel to match the other parameters, but set the tunnel wall

thickness w to 0.3m. To analyze the practical application performance of the GA-SVM model, a comparative analysis of path loss across different tunnels was conducted, including the Floating Interception (FI) model, Shooting and Bouncing Rays (SBR) model, and Ray Tracing with Alpha-Beta-Gamma (RT-ABG) model. The path loss is shown in Fig. 7.

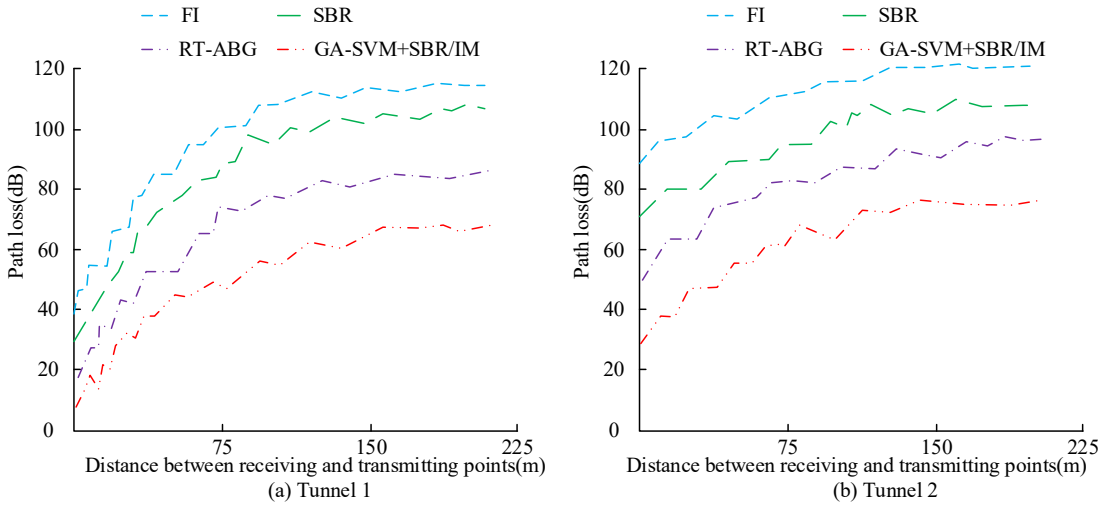


Fig. 7. Comparison of path losses in different tunnel walls

In Fig. 7(a), the fusion model GA-SVM+SBR/IM, with a tunnel wall thickness of 0.2m, had lower path loss values, with the highest value being only 63dB. However, the FI model had a higher path loss value of 114dB, which was 51dB higher than that of the fusion model. The fusion model used in tunnel 1 had lower path loss for 5G signals. In Fig. 7(b), at a tunnel wall thickness of 0.3m, the fusion model achieved a maximum path loss of 72dB, which was 9dB higher than that of tunnel 1. Meanwhile, the path loss value of the FI model could reach a maximum of 120dB, which was 6dB higher than that of tunnel 1. The thickness of the tunnel wall can significantly increase signal path loss, affecting signal propagation. The study compared the transmission signal-to-noise ratio (SNR) of different models, as shown in Fig. 8.

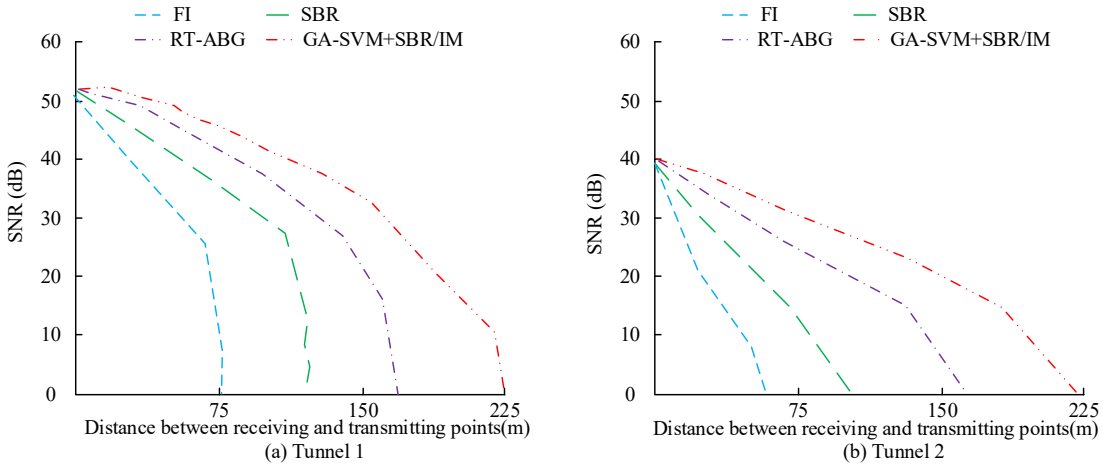


Fig. 8. SNR test results of different models

In Fig. 8(a), in tunnel 1, the fusion model reduced its SNR to 0dB only at about 225m from the transmission point. However, the FI model reduced its SNR to 0dB at 75m from the transmission point, indicating poor reception performance for communication signals and reduced accuracy, as the signal contains a large amount of noise. In Fig. 8(b), in tunnel 2, the SNR of the fusion model decreased to 0dB at about 220m from the transmission point, while the SNR of the FI model decreased to 0dB at 59m from the transmission point. This indicates that as the tunnel wall thickness increases, the impact on the 5G signal becomes more significant, and overall signal reception experiences more noise. The study compared the Received Signal Strength (RSSI), RMS Delay Spread, and Coherent Bandwidth of different models, as denoted in Table 1.

In Table 1, the performance of the fusion model used in different model comparisons was relatively better, with a relatively high acceptance strength, which was 7dBm higher than that of the FI model. Tunnel 1 was 20dBm higher than that of tunnel 2. In the comparison of coherence widths, the fusion model achieved a coherence width of up to 25 MHz, which was 10 MHz higher than that of the FI model. The value of tunnel 1 was significantly higher than that of tunnel 2, indicating that the tunnel wall will significantly affect 5G signal propagation. Using the studied fusion model can significantly improve the propagation of communication signals, enabling better reception and analysis.

Table 1. Comparison of 5G signal propagation performance among different models

Model	Metric	Tunnel 1	Tunnel 2
FI	Coherence Bandwidth	15MHz	8MHz
	RSSI	-75dBm	-95dBm
	RMS Delay Spread	35ns	70ns
SBR	Coherence Bandwidth	18MHz	10MHz
	RSSI	-72dBm	-92dBm
	RMS Delay Spread	30ns	65ns
RT-ABG	Coherence Bandwidth	22MHz	12MHz
	RSSI	-70dBm	-90dBm
	RMS Delay Spread	25ns	55ns
GA-SVM+SBR/IM fusion model	Coherence Bandwidth	25MHz	15MHz
	RSSI	-68dBm	-88dBm
	RMS Delay Spread	20ns	50ns

3.2. Model Generalization Performance Test Results

To analyze the reception and analysis effects of 5G signals after introducing different modules, the performance of integrating these modules was compared, as shown in Fig. 9. The simulation parameters are consistent with those used in the previous section.

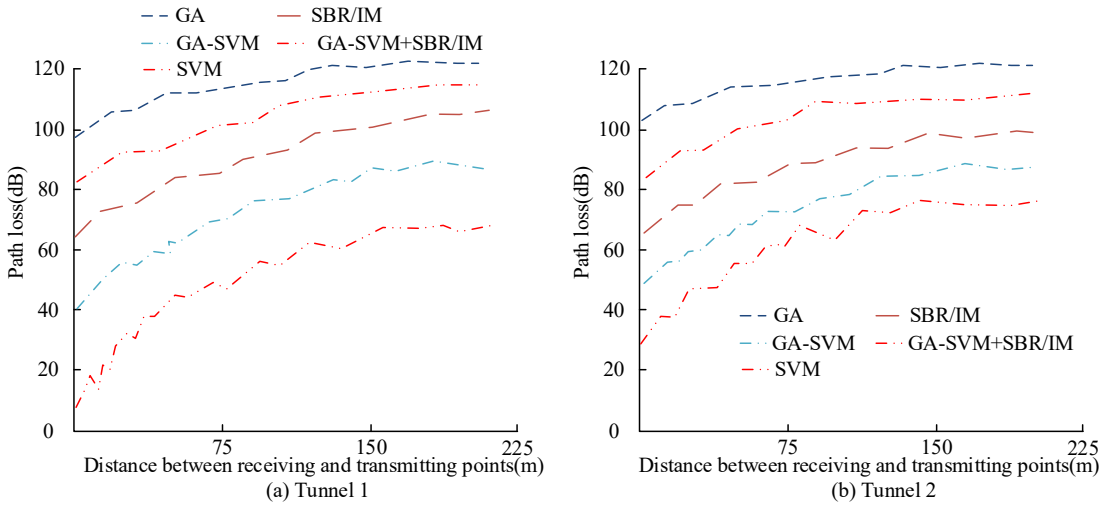


Fig. 9. Comparison of fusion model performance testing

In Fig. 9(a), the model's performance improved significantly after introducing different modules during tunnel 1 testing. Among them, the GA model had the worst performance, with the highest path loss value reaching 119dB, which was 56dB higher than that of the fused model. Meanwhile, the path loss of the GA-SVM model could reach 82dB without using SBR/IM, which was 19dB higher than that of the fused model. Using SBR/IM can significantly reduce signal path loss. In Fig. 9(b), after the thickening of the tunnel wall, there is no significant difference in the path loss values of the model before fusion, which may be due to the relatively small impact of the tunnel wall on the model before fusion. The study compared the transmission SNRs of different models, as shown in Fig. 10.

In Fig. 10(a), before fusing the different models, the GA model had the worst performance, with the SNR reduced to 0dB when the received signal was 46m. Compared with the fused model, the pre-fusion model performed relatively poorly and could not detect 5G electromagnetic signals either. Before fusing the SBR/IM model, the SNR of the GA-SVM model decreased to 0 at a receiving distance of about 200m, indicating that the GA-SVM model already had good signal analysis performance before fusing the model. From Fig. 10(b), there is no significant change in the transmission SNR of the model before fusion after the increase in tunnel wall thickness. This indicates that the transmission SNR of the unfused model changes little and does not significantly affect 5G signals. The performance of the base station network designed for research was analyzed, as denoted in Table 2.

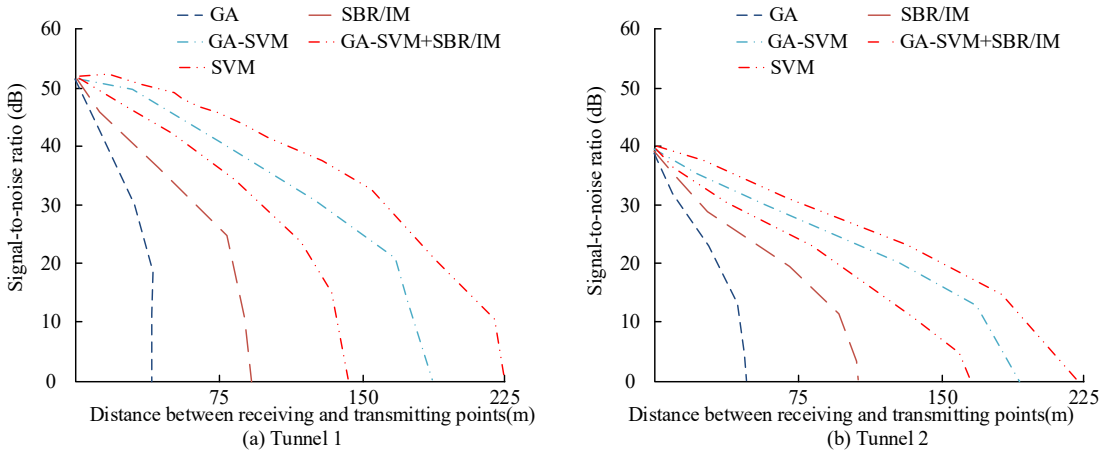


Fig. 10. Comparison of transmission SNRs of different models before fusion

Table 2. Performance analysis results of base station networks with different models

Model Name	Signal Strength (dBm)	Throughput (Mbps)	Delay (ms)	Jitter (ms)	Coverage Radius (m)
FI model	-85	120	45	12	90
SBR	-78	180	28	8	120
RT-ABG	-75	220	22	6	140
GA	-80	150	35	10	110
SVM	-77	190	30	7	125
GA-SVM	-73	250	20	5	150
SBR/IM	-72	280	18	4	160
GA-SVM+SBR/IM fusion model	-68	320	15	3	180

In Table 2, the fusion model had better network performance, with signal strength reaching -68 dBm, throughput reaching 320 Mbps, delay of only 15ms, minimum jitter of only 3ms, and signal coverage radius of up to 180 m. The fusion model could effectively combine the high-precision electromagnetic propagation simulation capability of the SBR/IM method with the intelligent optimization advantage of GA-SVM, and most accurately simulate the 5G signal propagation characteristics in coal mine tunnels. In the data comparison, each performance index of the traditional FI model was relatively poor, while the performance of the single models GA, SVMSBR, etc. was better than that of the traditional FI model but lower than that of the fusion model. The model's ability to analyze signal propagation characteristics can be significantly improved by fusing multiple models.

4. Conclusion

To analyze the propagation characteristics of 5G signals in coal mine tunnels, a method integrating SBR/IM and GA-SVM was proposed. This method used SBR/IM to build a 5G signal propagation model and GA-SVM to receive and analyze 5G signals, thereby characterizing their propagation in tunnels. The research results showed that when the wall thickness was 0.2m, the fusion method had a maximum path loss of only 63dB, while the FI model could reach a maximum of 114 dB, a difference of 51dB. This indicated that the fusion model significantly reduced the path loss of 5G signals. After increasing the wall thickness to 0.3m, the fusion model loss increased to 72dB, and the FI model loss could reach up to 120dB, indicating that increasing the wall thickness will significantly exacerbate signal attenuation. In the SNR analysis, the fusion model for tunnel 1 reduced the SNR to 0dB at 225m, whereas the FI model reduced it to 0dB only at 75m. The SNR of the fusion model in tunnel 2 decreased to 0dB at 220m, and the SNR of the FI model decreased to at 59m. The FI model's noise suppression was poor, and increasing wall thickness would further reduce signal reception quality. The RSSI of the fusion model was 7 dBm higher than that of the FI model, the coherence bandwidth was 10 MHz higher, and the overall performance of tunnel 1 was better than that of tunnel 2. Before the fusion model, the maximum path loss of GA could reach 119dB, and the maximum path loss of GA-SVM could reach 82dB. However, after introducing SBR/IM, the path loss was significantly reduced. The fusion model could achieve excellent performance with a minimum signal strength of -68 dBm, a throughput of 320 Mbps, a time delay of 15ms, and a coverage radius of 180m. The fusion model can significantly improve the propagation performance of 5G signals in tunnels and more effectively analyze their propagation characteristics. Although some achievements have been made in this research, there are still shortcomings, such as the analysis of only the tunnel wall thickness. Different data parameters will need to be analyzed in the future. This study only

analyzed some commonly used models. Therefore, more advanced models will need to be analyzed in the future. Based on the findings, managers should revise three key decisions. First, they should adopt a fusion model for path-loss prediction rather than empirical models, thereby enabling more accurate base-station placement and reducing coverage redundancy. Second, the significant impact of wall thickness on attenuation necessitates adjustments to inter-station spacing and received-signal strength thresholds during site planning. Third, the model's superior coherence bandwidth and low delay allow managers to confidently deploy high-order modulation and real-time control services, reallocating network resources away from conservative guard bands. These changes lead to more reliable and cost-effective 5G deployments in coal mine tunnels.

Funding

This research received no specific financial support from any funding agency.

Institutional Review Board Statement

Not applicable.

Declaration of Artificial Intelligence (AI) Tools

The authors used DeepSeek only for language editing and formatting assistance. The authors reviewed and took full responsibility for all content.

References

Bao, W., Xu, K., and Leng, Q. (2024). Research on the Financial Credit Risk Management Model of Real Estate Supply Chain Based on GA-SVM Algorithm: A Comprehensive Evaluation of AI Model and Traditional Model. *Procedia Computer Science,* 243(1), 900–909. DOI: 10.1016/j.procs.2024.09.108

Gai, L., Zhao, H., Li, X., Wang, P., Yu, S., Chen, Y., Wang, C., Lan, D., Han, F., and Du, Y. (2024). Shell engineering afforded dielectric polarization prevails and impedance amelioration toward electromagnetic wave absorption enhancement in nested‐network carbon architecture. *Chemical Engineering Journal,* 501(11), 157556–157557. DOI: 10.1016/j.cej.2024.157556

Guo, Z., Ren, J., Xu, X., Lan, D., Zhang, S., He, M., Gao, Z., Jia, Z., and Wu, G. (2025). Multiphase Co/Ni metal nitrides with heterointerfaces for enhanced interfacial polarization loss in electromagnetic wave absorption. *Journal of Materials Science & Technology*, 236(10), 19–27. DOI: 10.1016/j.jmst.2025.03.020

He, L., Xu, H., and Wang, X. (2024). Space-Confined multiple interface in super-structured TiO2@ PPy composite for enhanced electromagnetic wave absorption. *Applied Surface Science*, 646(10), 158898–158899. DOI: 10.1016/j.apsusc.2023.158898

Huang, L., Zhao, R., Ji, L., and Ruan, J. (2024). Chiral composite metamaterials with gradient phase index for vortex electromagnetic− wave generation and attenuation. *Journal of Alloys and Compounds,* 976(5), 173256–173257. DOI: 10.1016/j.jallcom.2023.173256

Kurbah, M. G. and Ahmed, F. (2024). Electromagnetic wave propagation in Eddington-inspired Born–Infeld gravity space-time with topological defects. The European Physical Journal C, 84(9), 903–904. DOI: 10.1140/epjc/s10052-024-13299-z

Lei, L., Wan, B. F., Liao, S. Y., and Zhang, H. F. (2024). Broadband asymmetric absorption-transmission and double-band rasorber of electromagnetic waves based on superconductor ceramics metastructures-photonic crystals. *Engineering Science and Technology, an International Journal,* 57(10), 101810–101811. DOI: 10.1016/j.jestch.2024.101810

Li, Y., Ren, P., Chen, R., Xu, B., and Wang, M. (2024). Design of miniaturized frequency selective rasorber based on complementary bandpass FSS for 5G applications. *IEEE Transactions on Electromagnetic Compatibility,* 66(2), 636–639. DOI: 10.1109/TEMC.2024.3363185

Liu, G., Zhu, P., Teng, J., Xi, R., Wang, X., Wang, X., Yan, M., and Wu, C. (2025). Optimizing MOF‐Derived Electromagnetic Wave Absorbers through Gradient Pore Regulation for Pareto Improvement. *Advanced Functional Materials,* 35(18), 2413048‐2413049.

Ma, Z., Li, X., and Sun, J. (2024). A data-driven fault detection approach for unknown large-scale systems based on GA-SVM. *Information Sciences*, 658(10), 120023–120024. DOI: 10.1016/j.ins.2023.120023

Ren, X., Sha, A., Jiang, W., Wu, W., Jiao, W., Li, J., and Li, J. (2024). Effect of EVA on the rheological properties of SBR-modified asphalt binder and its behavioral evolution during the thermo-oxidative aging process. *Construction and Building Materials,* 454(10), 139159–139160. DOI: 10.1016/j.conbuildmat.2024.139159

Shi, D., Li, W., Cui, K., Lian, C., Liu, X., Qi, Z., Xu, H., Zhou, J., Liu, Z., and Zhang, H. (2024). Electromagnetic radiation estimation at the ground plane near fifth‐generation base stations in China using a machine learning method. *IET Microwaves, Antennas & Propagation, 18*(6), 391–401. DOI: 10.1049/mia2.12467

Srinivas, J., Jagatheeshwaran, M. S., Vishvanathperumal, S., and Elayaperumal, A. (2025). A comparative study on the influence of nanoclay and nanosilica on the mechanical properties of NR/SBR/NBR ternary rubber nanocomposites. *Journal of Polymer Research,* 32(5), 187–188. DOI: 10.1007/s10965-025-04411-2

Su, X., Zhang, Y., Wang, J., and Liu, Y. (2024). Enhanced electromagnetic wave absorption and mechanical performances of graphite nanosheet/PVDF foams via ice dissolution and normal pressure drying. *Journal of Materials Chemistry C,* 12(21), 7775–7783. DOI: 10.1039/D4TC00929K

Wang, X., Cao, X., Ding, E., Yin, M., Huang, L., and Zhang, L. (2024). Kapok fiber-derived hollow carbon structure decorated with hydrangea-like MoS2 as sustainable and efficient electromagnetic wave absorbing composite fibers. *Carbon,* 221(5), 118887–118888. DOI: 10.1016/j.carbon.2024.118887

Wei, Q., Ge, X., Liu, J., and Li, H. (2024). A study on the ambient electromagnetic radiation level of 5G base stations in typical scenarios. *Radiation Detection Technology and Methods,* 8(3), 1333–1341. DOI: 10.1007/s41605-024-00452-1

Yu, S., Wang, C., Chen, Z., Qiu, Z., Chu, C., Cheng, Y., Zeng, T. and Sun, A. (2024). Additive manufacturing of broadband electromagnetic wave absorbing materials: polymer-derived SiC/Si3N4 composites with triply periodic minimal surface meta-structure. *Chemical Engineering Journal,* 483(3), 149185–149186. DOI: 10.1016/j.cej.2024.149185

Zhang, Y., Wang, J., Wu, Q., Shan, T., Bai, S., Lan, D., Zhang, B., Liu, Y. and Su, X. (2025). Enhanced electromagnetic wave absorption of bacterial cellulose/reduced graphene oxide aerogel by eco-friendly in-situ construction. *Journal of Colloid and Interface Science,* 678(1), 648–655. DOI: 10.1016/j.jcis.2024.08.211

Zhu, J., Lan, D., Liu, X., Zhang, S., Jia, Z., and Wu, G. (2024). Porous structure fibers based on multi‐element heterogeneous components for optimized electromagnetic wave absorption and self‐anticorrosion performance. *Small,* 20(47), 2403689‐2403690. DOI: 10.1002/smll.202403689



Zhiguo Wen was born in 1988. He earned his Master of Engineering and is an Associate Research Fellow. He received his bachelor's degree from China University of Mining and Technology in 2012. Received a master's degree from the China Coal Research Institute in 2015. He is currently the Director of the Hydraulic Power Research Institute at the Intelligent Equipment Branch of China Coal Technology and Engineering Group Co., Ltd. His research interests currently focus on automation and intelligent monitoring technologies for comprehensive coal mining equipment.